Size and functional tuning of solid state nanopores by chemical functionalization

2012 Nanotechnology 23 435301

(http://iopscience.iop.org/0957-4484/23/43/435301)

Nanotechnology **23** (2012) 435301 (8pp) doi:10.1088/0957-4484/23/43/435301

Size and functional tuning of solid state nanopores by chemical functionalization

Valentina Mussi, Paola Fanzio, Giuseppe Firpo, Luca Repetto and Ugo Valbusa

Nanomed Labs, Physics Department, University of Genova, Via Dodecaneso, 33 Genova, I-16146, Italy

E-mail: mussi@fisica.unige.it

Received 21 April 2012, in final form 17 July 2012
Published 11 October 2012
Online at stacks.iop.org/Nano/23/435301

Abstract
We demonstrate the possibility of using a simple functionalization procedure, based on an initial vapour-phase silanization, to control the size and functionality of solid state nanopores. The presented results show that, by varying the silanization time, it is possible to modify the efficiency of probe molecule attachment, thus shrinking the pore to the chosen size, while introducing a specific sensing selectivity. The proposed method allows us to tune the nanopore biosensor adapting it to the specific final application, and it can be efficiently applied when the pore initial diameter does not exceed a limit dimension related to the mean free path of the silane molecules at the working pressure.

(Some figures may appear in colour only in the online journal)

1. Introduction

Nanopore technology is a growing and spreading research field, which covers many different areas, from single molecule stochastic sensing [1, 2] to medical screening and diagnosis [3, 4], and therefore plays an important role at the forefront of biotechnology and life science. Nanopore based devices, both biological [5] and synthetic [6], allow us to detect and interrogate single molecules by monitoring the modulation of the pore electrical conductance. This simple transduction mechanism is particularly powerful because it allows us to reduce the necessary sample volume and concentration, greatly decrease time and cost of the analysis, avoid labelling and mimic basic biological functionalities [7]. Such devices have already been successfully used to count, sort and manipulate different kinds of molecules and biopolymers [8, 9], to study protein folding and unfolding [10], to investigate biomolecular interactions [11, 12], and they have also been proposed for use in ultra-rapid DNA sequencing [13, 14] and gene expression profiling [15]. In most cases, the information is obtained by simply registering and analysing the transient ionic current reduction induced by the physical obstruction of the nanochannel caused by the molecule translocation. However, even if this 'resistive pulse technique' [16] allows us to maximize the sample processing speed, avoiding specific target preparation, most of the present efforts aim to develop smart sensors, with proper selectivity and specific chemical and biological functionalities [17, 18]. Protein nanopores have been, in fact, modified by replacement or substitution of amino acids for stochastic sensing of metal ions [19], engineered by covalent attachment of probe molecules to sense target DNA molecules or proteins [20] and also equipped with noncovalent adapters, to allow the specific binding of analytes [21]. To overcome the limitations of biological pores, which suffer from a fixed geometry and limited lifetime and stability, solid state nanopores and nanochannels have been introduced and realized in silicon materials [22], polymers [23, 24], glass [25], metals [26, 27] and graphene [28]. These synthetic counterparts of protein pores have adjustable size, shape and surface properties, and can be integrated into complex lab-on-a-chip devices, hence enhancing their technological applicability. Nevertheless, they are non-selective and chemically inert. Many strategies have been so far introduced to chemically modify their surface with organic coatings, in order to confer on them sensing selectivity [22, 29, 30]. For instance, self-assembled organosilane coating was used to control the pH response of silicon nitride pores [31] and to functionalize them with amino-terminated molecules [32–34]. The nanopore is frequently modified by a procedure involving surface

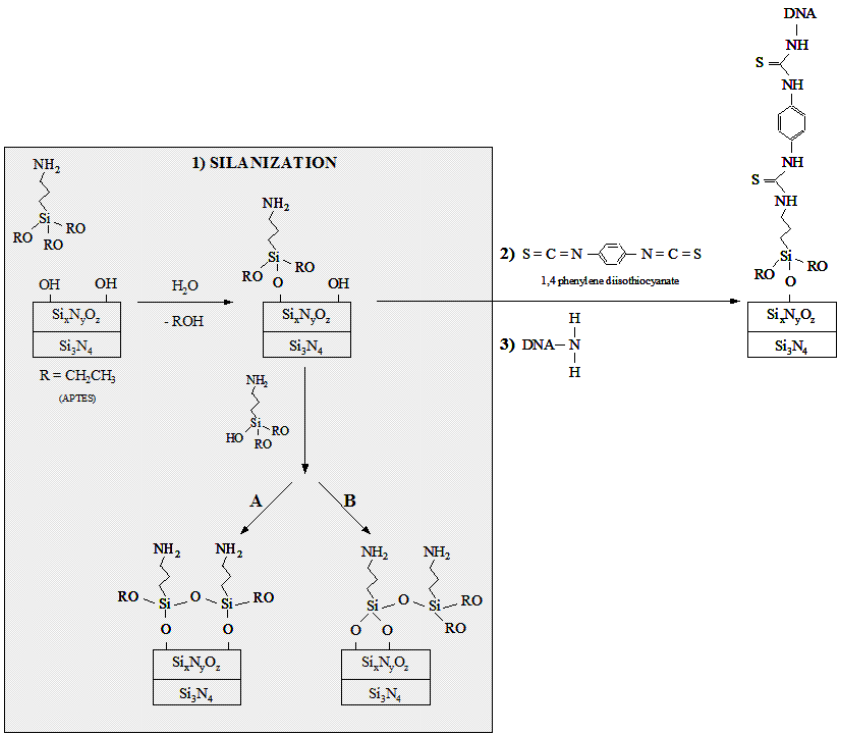

Figure 1. Scheme of the three-step functionalization procedure of the nanopores. The first step (silanization) is evidenced in the grey box. Due to the water molecules present on the nanopore surface, silanes can deposit not only as an ordered layer (bottom-left arrow, (A)) but also as a vertical more complex structure by self-polymerization (bottom right arrow, (B)). The second step of the procedure (number 2 on the centre of the figure) consists of a liquid-phase treatment with 1,4-phenylene diisothiocyanate cross-linker. Then, an over-night treatment with amino-modified DNA is performed (step number 3 in the centre of the figure). The functionalized chip is represented as a final product on the right of the figure.

silanization followed by the attachment of an intermediate cross-linker and the specific probe molecule. This is a quite general approach, which exploits the silanol groups present on the silica surface, and it is widely used to alter the surface properties of inorganic materials in order to increase cell adhesion [35], to immobilize proteins for immunoassays [36], for DNA chips [37] and high resolution imaging of biomolecules [38]. However, while the functionalization of planar surfaces for biosensing has been extensively investigated, the functionalization of nanometric structures still remains a challenging and complex issue [39, 40]. We recently demonstrated that, by functionalizing a nanopore with oligonucleotides, it is possible to simultaneously resize and activate it [41, 42]. Functionalized nanopores are characterized by a reduced effective pore diameter (EPD) [43] depending on contour length, stiffness and total charge of the used probe molecules, i.e. on their re-orienting and stretching under the external electric field. As underlined in [33, 43, 44], this is a very crucial point for many advanced applications, such as DNA analysis and sequencing. A number of solutions have been identified to tailor the EPD: controlling the bare nanopore size during fabrication [45] (also post-depositing oxide layers on the surface, [32, 33]), carefully choosing the probe molecules, adjusting the strength of the applied electric field [43], and altering the persistence length of the DNA probe molecules by modifying the ionic concentration of the solution [46]. In the present paper, we introduce a new approach to tune the EPD of the pore. The proposed procedure uses vapour-phase silanization with a variable duration to regulate the thickness of the organic coating, so adapting the device to the application and target molecule. Specifically, we use 3-aminopropyl triethoxy silane (APTES) because it is highly reactive, and can give rise to a number of possible surface structures [47]. Its attachment on silica is, in fact, driven by an initial hydrolysis that can occur either in solution, or at the substrate surface, depending on the amount of water present [48]. The interaction with surface silanol groups (SiOH) results in siloxane bonding (Si–O–Si), accompanied by ROH as a by-product (R = CH_2CH_3). It is then possible to produce ordered self-assembled monolayers (SAMs), but self-polymerization of APTES in solution usually prevents the formation of homogeneous films, causing polysiloxane deposition at the surface, due to 3D vertical polymerization [47]. This partial vertical polymerization of silane molecules can be interestingly exploited to control the resizing of nanostructures by chemical functionalization. In particular, the formation of thick layers of coupling molecules induced by small amounts of surface water can be used to attach oligonucleotides to solid state nanopores, so to produce selective, tunable and sensitive biosensors. For this purpose, we tested a three-step procedure based on the vapour-phase silanization suggested in [49] and illustrated in figure 1 (details are given in section 2). Data presented here prove that, by varying the silanization time, it is possible to modify the functionalization efficiency, thus tuning the thickness of the organic coating, i.e. the size of the nanopore,

while adjusting the biosensor functionality and selectivity. This quite simple preparation method, being applicable with many different probe molecules, i.e. for a range of different targets, is very powerful and versatile. As shown here, its efficient application requires a careful consideration of the parameters influencing the process of chemical modification of nano-confined regions, a fundamental issue for many advanced applications of nanopore technology.

2. Experimental details

2.1. Nanopore fabrication

A thin (20–100 nm nominal thickness) SiN film is deposited on a 300 μm thick Si substrate. The Si side of the chip is then anisotropically etched until a silicon nitride area 80 $\times$ 80 μm^2 large is exposed. Nanopores are fabricated on this free-standing membrane using a CrossBeam® workstation model 1540XB (Carl Zeiss AG, Oberkochen, Germany) that combines an ultra-high resolution scanning electron microscope (UHR-SEM) and a focused ion beam (FIB), and is equipped with a scanning transmission electron microscopy (STEM) detector. The pore drilling is made by exposing the membrane for 1 s to a resting and focused ion beam of 2 pA.

2.2. Nanopore functionalization

The Si/SiN chip is initially subjected to an oxygen plasma treatment (60 s, 30 W) to clean any organic contamination and produce hydroxyl groups on the SiN surface. As illustrated in figure 1, the subsequent functionalization procedure consists of three main steps. First of all, the chip is exposed to silanes in vapour phase by placing it inside a dynamically pumped low vacuum chamber near to a glass holder containing 20 μl of APTES (Sigma-Aldrich), at ambient temperature and base pressure $P \sim 30$ kPa. This first step (silanization) is evidenced in the grey box in figure 1. Due to the water molecules present on the nanopore surface, silanes can deposit not only as an ordered layer (bottom-left arrow, (A)) but also as a vertical more complex structure by self-polymerization (bottom right arrow, (B)). The second step of the procedure (number 2 in the centre of figure 1) consists of a liquid-phase treatment with 1,4-phenylene diisothiocyanate cross-linker (0.5% P/V in dimethyl sulfoxide) for 1 h followed by two washes in dimethyl sulfoxide and two washes in double distilled water. Finally, an over-night treatment at 37 °C with 100 nM amino-modified DNA (5′-GCC AAA AGG GTC ATC ATC TCT GCC CCC TCT GCT GAT GCC CCC ATG-3′ sequence, MWG Biotech, Germany) in ddH_2O pH 8–9 is performed (step number 3 in the centre of figure 1), followed by two washes with 28% ammonia solution and by two washes with ddH_2O to de-activate the substrate.

2.3. SEM and STEM imaging

SEM images of the nanopores, before and after the functionalization, are obtained by using an accelerating voltage of 20 kV and an aperture size of 30 μm. The sample is placed at 2 mm working distance, and the in-lens detector is used to image surface structures. The images are taken at a scan rate with a dwell time of 6.4 μs, averaging over 10 line scans, so as to obtain a good signal to noise ratio. In these conditions, SEM artefacts are minimized, carbon deposition above all, and, despite the sample being non-conductive, there is no drift of the electron beam.

STEM imaging of the nanopores, before and after the functionalization, is obtained by using an accelerating voltage of 30 kV in bright field mode.

2.4. Electrical measurements

To perform electrical measurements, both before and after the functionalization procedure, the nanopored chips are mounted between rubber gaskets in a microfluidic cell placed in a double Faraday cage enclosure on an anti-vibration table. The cell is made of two facing plexiglas chambers filled with filtered 1 M KCl ionic solution (conductivity $\sim$ 10 S m^{-1}, pH = 7). Two Ag/AgCl pellet electrodes (Warner Instruments, E206) are used to apply a voltage bias and collect the ion current by means of a patch-clamp amplifier (Axopatch 200B, Axon Instruments, 250 kHz sampling rate, low-pass four-pole Bessel filter set at 10 kHz).

3. Results and discussion

Different nanopores with similar initial diameter (about 80 nm) were functionalized by just varying the duration of the vapour-phase silanization step (that is the part of the procedure contained in the grey box of figure 1) while maintaining unaltered both the sequence of steps depicted in section 2.2 and the external parameters. The reaction occurs very quickly, so that the time of exposition to the silane molecules, t_e, was set between 60 and 420 s. At the end of the functionalization procedure, after the attachment of the oligonucleotides, the chips, represented as a final product on the right of figure 1, were analysed by SEM imaging, to point out the surface modifications induced in the nanopore area by the chemical activation. The collected SEM images are shown in figure 2 for a non-functionalized nanopore ($t_e = 0$ s), and five nanopores treated with silanes for $t_e = 60$ s, 180 s, 240 s, 300 s and 420 s, respectively. The presence of the organic layer is associated to the appearance of a ragged edge on the circular pore, and, as evident in figure 2, it depends on the silanization time: 60 s are not sufficient to produce noticeable modifications, but once the silane film starts covering the nanopore surface, the binding of biomolecules becomes more and more efficient, producing a progressive shrinking of the diameter. In this regards, the final effect of the 300 and 420 s silanization treatment is quite similar, consisting in an almost complete coverage of the nanopore aperture with the probe molecules, and resulting in an organic layer having a thickness (20–23 nm, as deduced by SEM images) slightly larger than the contour length of the used oligonucleotides (45 bases, corresponding to about 15 nm). This result is consistent with a functionalization which is not initiated with the formation of a simple monolayer of silane molecules. For $t_e \geq 600$ s,

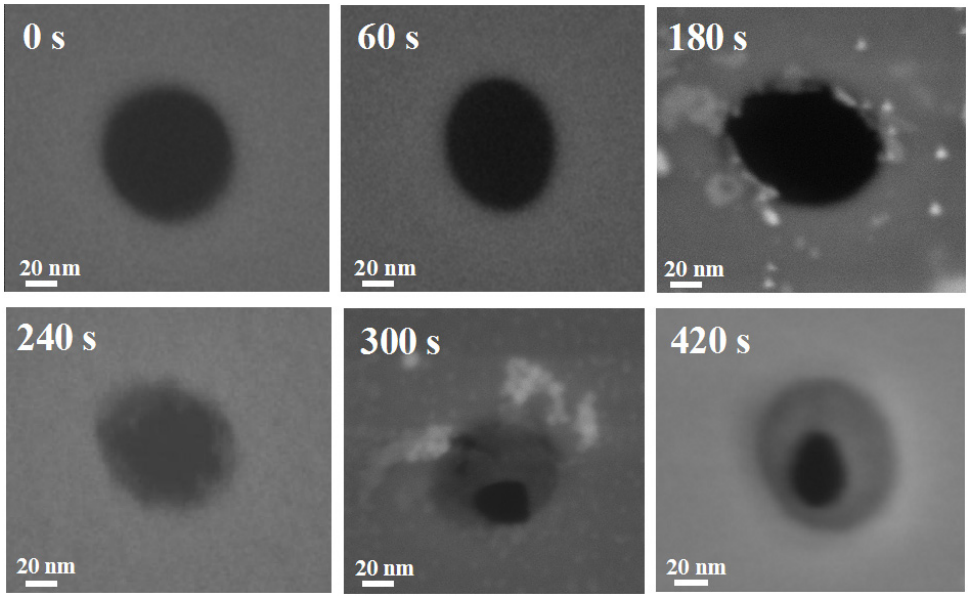

Figure 2. SEM images (accelerating voltage of 20 kV and aperture size of 30 μm) obtained on, respectively, a non-functionalized nanopore (silanization time $t_e = 0$ s) and five nanopores treated with silanes for $t_e = 60$, 180, 240, 300 and 420 s. The presence of the organic layer is associated to the appearance of a ragged edge on the circular pore, and depends on t_e.

almost all the nanopores appear clogged to the SEM analysis, indicating a progressive disordered linking and superposing of the probe molecules that causes the fouling of the nanometric aperture.

As shown in figure 3, this resizing behaviour is nicely confirmed by electrical measurements performed on a series of nanopored chips functionalized by using different silanization times. For each nanopore, a voltage–current curve was measured both before and after the probe attachment, and a linear fit was used to estimate the electrical resistance. As an example, figure 3(A) presents the voltage–current curves obtained on the same chip before and after the chemical modification produced by using a 240 s silanization. The measured relevant increase in the electrical resistance from about $R = 5.5$ MΩ, for the bare nanopore (NP), to about $R_f = 21.2$ MΩ, for the functionalized nanopore, is caused by the size reduction produced by the probe attachment. In fact, the values of R/R_f reported in figure 3(B) as a function of the silanization time, allow us to estimate the continuously growing percentage reduction of the pore area with the thickness of the organic coating. As shown in the figure, the revealed behaviour can be fit by an exponential decay with a single time constant of 116 s, whose value is likely related to the pressure and temperature conditions used during the silanization. Even if an exact analysis of the dynamics of the process will require further investigation, electrical measurements clearly demonstrate the possibility of building a specific calibration curve for the pore resizing. We further tested the reproducibility of the procedure by means of STEM imaging. Figure 4(A) presents a STEM image realized on a pore having similar dimension with respect to those used for electrical measurements. The enhanced contrast between the electron transmitting and not transmitting regions permits a fine determination of the initial area. Similarly, the STEM image realized on the pore after the functionalization obtained by using a 300 s silanization, shown in figure 4(B), allows us to precisely distinguish the residual open area from the region covered by the probe molecules (grey reticulated area). The analysis performed on the STEM image gives an estimation of the ratio between the open areas after and before the functionalization of 0.14, which is a value in good agreement with the electrical estimation of 0.16 obtained for 300 s silanization (see figure 3(B)).

The preparation procedure thus requires precise control of the first activation step, which is highly dependent on the chosen probe molecules and on the final diameter needed for the specific application, but is extremely simple and effective, enabling a very fast realization of a selective solid state nanopore biosensor. Such kinds of functionalized pores have been successfully used to perform translocation experiments of long dsDNA molecules, thanks to the sensitivity acquired through the diameter reduction, and hybridization experiments with complementary target sequences, thanks to the selectivity of the interaction between the probe attached to the sensor surface and the dispersed target molecules [50].

The use of the chemical functionalization to tune both the size and the functionality of the nanopore biosensors, enables us to elaborate a manufacturing strategy which does not require, in principle, a very demanding nano-fabrication technique. As demonstrated by the data reported in figures 2–4, nanopores with a quite large initial diameter of about 60–80 nm can be, in fact, modified and resized to be used for single molecule sensing. One might wonder to what extent this mechanism is flexible: is it possible to start from even larger pores, having dimension compatible with lithographic techniques, and still obtain functional biosensors? To test this hypothesis we prepared a Si/SiN chip containing a

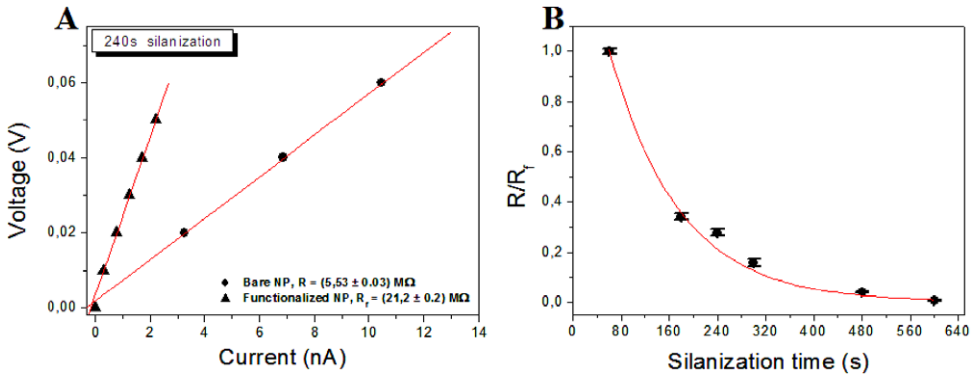

Figure 3. Electrical measurements performed on a series of nanopored chips functionalized by using different silanization times. As an example, (A) presents the voltage–current curves obtained on the same chip before and after the chemical modification produced by using a 240 s silanization. A linear fit allows us to estimate a relevant increase in the electrical resistance from about $R = 5.5$ MΩ, for the bare nanopore (NP), to about $R_f = 21.2$ MΩ, for the functionalized nanopore, caused by the size reduction produced by the probe attachment. (B) Reports the values of R/R_f as a function of the silanization time, showing a continuously growing percentage reduction of the pore area with the thickness of the organic coating.

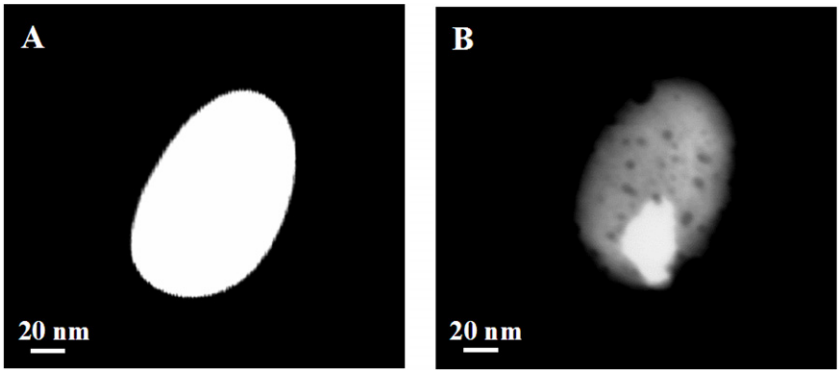

Figure 4. STEM images (accelerating voltage of 30 kV, bright field mode) realized on the same nanopore before, (A), and after, (B), the functionalization obtained by using a 300 s silanization. The enhanced contrast between the electron transmitting and not transmitting regions permits us to precisely distinguish, for the functionalized pore, the residual open area from the region covered by the probe molecules (grey reticulated area).

series of seven pores of increasing diameter, from 250 nm to about 2 μm. The chip was then subjected to the same functionalization procedure used for the nanopore of figure 4 ($t_e = 300$ s), and analysed by SEM imaging. The upper part of figure 5 presents a large scale image of the entire set of nanopores realized by FIB drilling on the SiN membrane. For each of them, two images are reported in figure 5: a numbered one (from 1 to 7), obtained on the pore before the treatment, and, immediately below, that collected after the functionalization. These images show that all the pores are clogged and coated with a layer of material whose thickness and density appear even to increase with the increase of the diameter, a result clearly not comparable with that obtained with smaller nanometric apertures. We ascribe this behaviour to the specific flow regime of the vapour-phase silanization process. Indeed, the pressure distribution inside the vacuum chamber during the exposition of the Si/SiN nanopored chip to the silanes, being dynamically generated, cannot be considered uniform, so that a pressure difference is present across the nanopore, allowing a gas flow through the orifice [51, 52]. The flow regime through the nanopore is determined by the ratio between the pore diameter d, and the molecule mean free path λ. The mean free path of a molecule depends on its diameter D, the temperature T and the pressure P according to the relationship:

$$\lambda = \frac{k_B T}{\sqrt{2}\pi D^2 P} \quad (1)$$

where k_B is the Boltzmann constant. By considering the parameters set during the functionalization, $P = 30$ kPa, $T \sim 25\,^{\circ}$C (see section 2.2), and the diameter of silane molecules, $D = 3.55$ Å [53], equation (1) gives an estimated mean free path $\lambda = 245$ nm. The silanization of the smaller nanopores of figures 2–4 hence occurs in the molecular flow regime ($d < 100$ nm $< \lambda$). The gas molecules follow independent trajectories and interact preferentially with the pores' surface, so that a controllable and tunable functionalization of the surface is possible [54]. Differently, the chemical modification of the larger pores of figure 5 takes place in a viscous flow regime ($d > 250$ nm $> \lambda$). In this case, the gas downstream from the orifice is dense, and the convergent flow towards the axis of the pore causes its clogging [54]. As a consequence, the functionalization cannot be steered, and rather requires a different setting of the parameters affecting λ. Similar

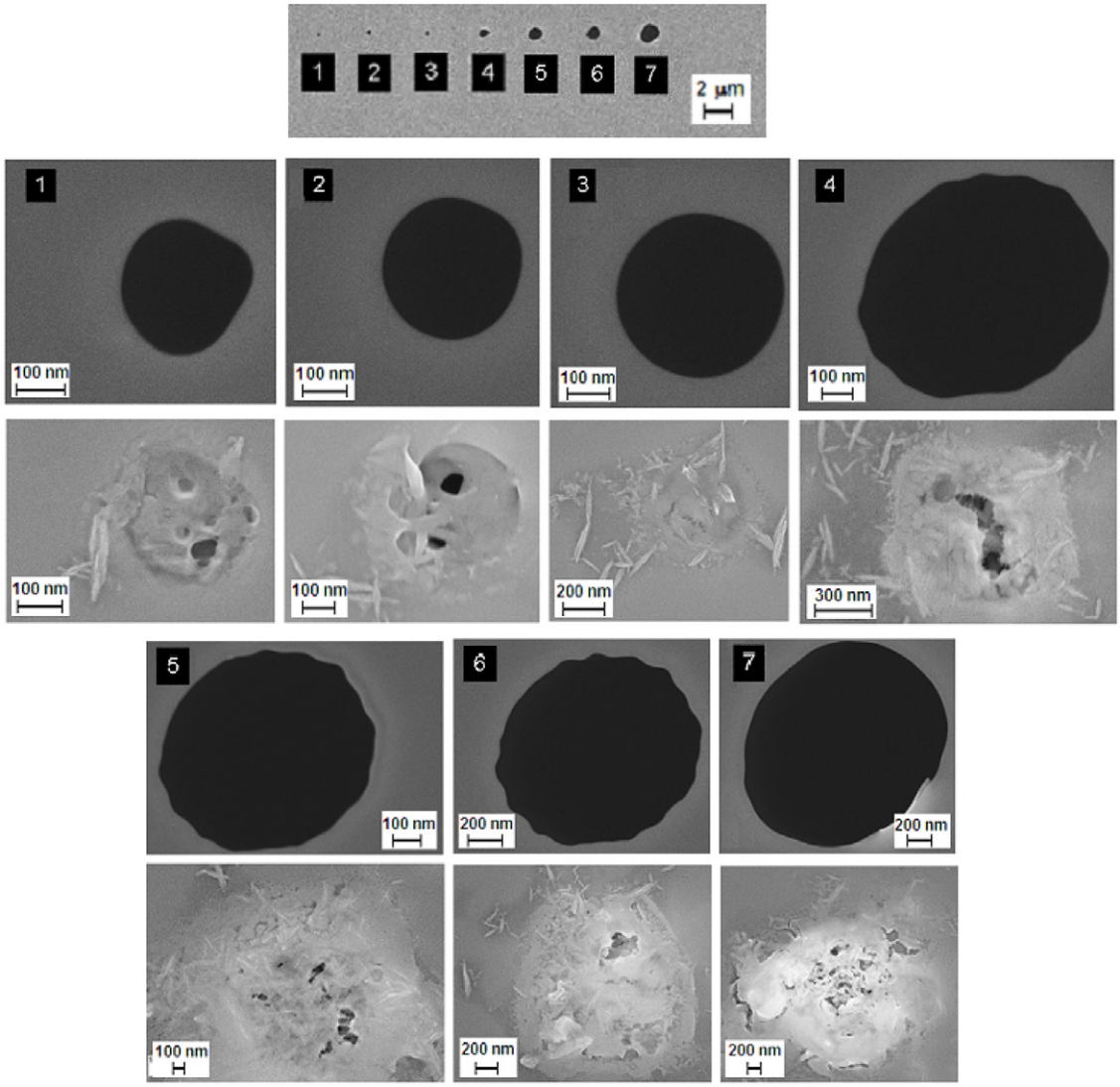

Figure 5. Upper part of the figure: large scale SEM image of a set of seven pores of increasing diameter, from 250 nm to about 2 μm, realized by FIB drilling on a SiN membrane. For each of them, two images are reported in the figure: a numbered one (from 1 to 7), obtained on the pore before the treatment, and, immediately below, that collected after the functionalization.

considerations have been used in the literature to control the process of nanoscale patterning of organosilane thin films directly from the gas phase, and are fundamental to the design and manufacture of multifunctional surfaces [55].

In conclusion, we demonstrated the possibility of using a simple functionalization procedure to produce effective single molecule biosensing devices by starting from FIB fabricated solid state nanopores. Our approach is based on the simultaneous tuning of pore size and functionality as induced by the chemical covalent attachment of probe biomolecules on its surface. The developed protocol does not involve a tough deposition of organic material, being based, instead, on a vapour-phase silanization of the entire chip surface. SEM and STEM imaging, and electrical measurements have been used to show that, by varying the silanization time, it is possible to control and tune the functionalization efficiency, thus shrinking the nanopore till the chosen size, while introducing a specific sensing selectivity. We found that, by using 45-mer oligonucleotides as probe molecules and 300 s of vapour-phase silanization at $P = 30$ kPa and ambient temperatures, it is possible to obtain the complete coverage of the nanopore aperture. Under these conditions, the functionalization produces an $\sim$80% size reduction of the pores, the process being driven by the vertical polymerization of the silane molecules. The great advantage of the proposed strategy is its simplicity and versatility. Indeed, being adaptable to different probe molecules, it allows the preparation of biosensors for a variety of different applications and target biomolecules. Finally, we verified that the process is only steerable for nanopores having an initial size less than the mean free path of the silane molecules at the working pressure. Under these conditions, the silane flow regime is molecular and the functionalization process is sufficiently ordered so as not to cause the rapid clogging of the nanometric aperture, which is a fundamental issue in the field of chemical modification of nano-confined regions for advanced biotechnological applications.

Acknowledgments

This work has been supported by Ministero dell'Università e della Ricerca (MIUR), Italy, with the National Project *Nanomax*. We thank Fondazione Bruno Kessler, FBK, for the Si/SiN chip fabrication and ElbaTech S.r.l. for the microfluidic cell construction.

References

[1] Zhao Q, Wang D, Jayawardhana D A and Guan X 2008 Stochastic sensing of biomolecules in a nanopore sensor array *Nanotechnology* **19** 505504
[2] Rosenstein J K, Wanunu M, Merchant C A, Drndic M and Shepard K L 2012 Integrated nanopore sensing platform with sub-microsecond temporal resolution *Nature Methods* **9** 487–92
[3] Venkatesan B M and Bashir R 2011 Nanopore sensors for nucleic acid analysis *Nature Nanotechnol.* **6** 615–24
[4] Mirsaidov U M, Wang D, Timp W and Timp G 2010 Molecular diagnostics for personal medicine using a nanopore *Wiley Interdiscip. Rev. Nanomed. Nanobiotechnol.* **2** 367–81
[5] Ma L and Cockroft S L 2010 Biological nanopores for single-molecule biophysics *ChemBioChem* **11** 25–34
[6] Healy K, Schiedt B and Morrison A P 2007 Solid-state nanopore technologies for nanopore-based DNA analysis *Nanomedicine* **2** 875–97
[7] Kowalczyk S W, Kapinos L, Blosser T R, Magalhães T, van Nies P, Lim R Y H and Dekker C 2011 Single-molecule transport across an individual biomimetic nuclear pore complex *Nature Nanotechnol.* **6** 433–8
[8] Li J and Golovchenko J A 2009 Solid-state nanopore for detecting individual biopolymers *Methods Mol. Biol.* **544** 81–93
[9] Kumar H, Lansac Y, Glassef M A and Maiti P K 2011 Biopolymers in nanopores: challenges and opportunities *Soft Matter.* **7** 5898–907
[10] Oukhaled G, Mathé J, Biance A L, Bacri L, Betton J M, Lairez D, Pelta J and Auvray L 2007 Unfolding of proteins and long transient conformations detected by single nanopore recording *Phys. Rev. Lett.* **98** 158101
[11] Dudko O K and Meller A 2009 Probing biomolecular interactions using nanopore force spectroscopy *Encyclopedia of Analytical Chemistry* ed R A Meyers (New York: Wiley)
[12] Balagurusamy V S K, Weinger P and Ling X S 2010 Detection of DNA hybridizations using solid-state nanopores *Nanotechnology* **21** 335102
[13] Cherf G M, Lieberman K R, Rashid H, Lam C E, Karplus K and Akeson M 2012 Automated forward and reverse ratcheting of DNA in a nanopore at 5-Å precision *Nature Biotechnol.* **30** 344–8
[14] Manrao E A, Derrington I M, Laszlo A H, Langford K W, Hopper M K, Gillgren N, Pavlenok M, Niederweis M and Gundlach J H 2012 Reading DNA at single-nucleotide resolution with a mutant MspA nanopore and phi29 DNA polymerase *Nature Biotechnol.* **30** 349–53
[15] Singer A, Wanunu M, Morrison W, Kuhn H, Frank-Kamenetskii M and Meller A 2010 Nanopore based sequence specific detection of duplex DNA for genomic profiling *Nano Lett.* **10** 738–42
[16] Bezrukov S M, Vodyanoy I and Parsegian V A 1994 Counting polymers moving through a single-ion channel *Nature* **370** 279–81
[17] Hou X, Guo W and Jiang L 2011 Biomimetic smart nanopores and nanochannels *Chem. Soc. Rev.* **40** 2385–401
[18] Kowalczyk S W, Blosser T R and Dekker C 2011 Biomimetic nanopores: learning from and about nature *Trends Biotechnol.* **29** 607–14
[19] Xie H, Braha O, Gu L Q, Cheley S and Bayley H 2005 Single-molecule observation of the catalytic subunit of cAMP-dependent protein kinase binding to an inhibitor probe *Chem. Biol.* **12** 109–20
[20] Howorka S and Siwy Z 2009 Nanopore analytics: sensing of single molecules *Chem. Soc. Rev.* **38** 2360–84
[21] Banerjee A, Mikhailova E, Cheley S, Gu L, Montoya M, Nagaoka Y, Gouaux E and Bayley H 2010 Molecular bases of cyclodextrin adapter interactions with engineered protein nanopores *Proc. Natl Acad. Sci.* **107** 8165–70
[22] Gyurcsányi R E 2008 Chemically-modified nanopores for sensing *Trends Anal. Chem.* **27** 627–39
[23] Mara A, Siwy Z, Trautmann C, Wan J and Kamme F 2004 An asymmetric polymer nanopore for single molecule detection *Nano Lett.* **4** 497–501
[24] Saleh O A and Sohn L L 2003 An artificial nanopore for molecular sensing *Nano Lett.* **3** 37–8
[25] Sha J, Ni Z, Liu L, Yi H and Chen Y 2011 A novel method of fabricating a nanopore based on a glass tube for single-molecule detection *Nanotechnology* **22** 175304
[26] Nagoshi K, Honda J, Sakaue H, Takahagi T and Suzuki H 2009 Direct fabrication of nanopores in a metal foil using focused ion beam with *in situ* measurements of the penetrating ion beam current *Rev. Sci. Instrum.* **80** 125102
[27] Nishizawa M, Menon V P and Martin C R 1995 Metal nanotubule membranes with electrochemically switchable ion-transport selectivity *Science* **5** 700–2
[28] Liu S, Zhao Q, Xu J, Yan K, Peng H, Yang F, You L and Yu D 2012 Fast and controllable fabrication of suspended graphene nanopore devices *Nanotechnology* **23** 085301
[29] Yusko E C, Johnson J M, Majd S, Prangkio P, Rollings R C, Li J, Yang J and Mayer M 2011 Controlling protein translocation through nanopores with bio-inspired fluid walls *Nature Nanotechnol.* **6** 253–60
[30] Ali M, Schiedt B, Neumann R and Ensinger W 2010 Biosensing with functionalized single asymmetric polymer nanochannels *Macromol. Biosci.* **10** 28–32
[31] Wanunu M and Meller A 2007 Chemically modified solid-state nanopores *Nano Lett.* **7** 1580–5
[32] Nillson J, Lee J R I, Ratto T V and Letant S E 2006 Localized functionalization of single nanopores *Adv. Mater.* **18** 427–31
[33] Iqbal S M, Akin D and Bashir R 2007 Solid-state nanopore channels with DNA selectivity *Nature Nanotechnol.* **2** 243–8
[34] Kim Y, Min J, Lee I, Kim S, Kim A, Kim K, Namkoong K and Ko C 2007 Nanopore sensor for fast label-free detection of short double-stranded DNAs *Biosens. Bioelectron.* **22** 2926–31
[35] Seitz O, Fernandes P G, Tian R, Karnik N, Wen H, Stiegler H, Chapman R A, Vogel E M and Chabal Y J 2011 Control and stability of self-assembled monolayers under biosensing conditions *J. Mater. Chem.* **21** 4384–92
[36] Wang Z and Jin G 2004 Covalent immobilization of proteins for the biosensor based on imaging ellipsometry *J. Immunol. Methods* **285** 237–43
[37] Halliwell C M and Anthony Cass E G 2001 A factorial analysis of silanization conditions for the immobilization of oligonucleotides on glass surfaces *Anal. Chem.* **73** 2476–83
[38] Karrasch S, Dolder M, Schabert F, Ramsden J and Engel A 1993 Covalent binding of biological samples to solid supports for scanning probe microscopy in buffer solution *Biophys. J.* **65** 2437–46

[39] Iqbal S M and Bashir R (ed) 2011 *Nanopores: Sensing and Fundamental Biological Interactions* (New York: Springer)
[40] Howorka S and Siwy Z S 2012 Nanopores as protein sensors *Nature Biotechnol.* **30** 506–7
[41] Mussi V, Fanzio P, Repetto L, Firpo G, Scaruffi P, Stigliani S, Tonini G P and Valbusa U 2010 DNA-functionalized solid state nanopore for biosensing *Nanotechnology* **21** 145102
[42] Mussi V, Fanzio P, Repetto L, Firpo G, Scaruffi P, Stigliani S, Menotta M, Magnani M, Tonini G P and Valbusa U 2010 Electrical characterization of DNA-functionalized solid state nanopores for bio-sensing *J. Phys.: Condens. Matter* **22** 454104
[43] Ramachandran A, Guo Q, Iqbal S M and Liu Y 2011 Coarse-grained molecular dynamics simulation of DNA translocation in chemically-modified nanopores *Phys. Chem.* B **115** 6138–48
[44] Peleg O, Tagliazucchi M, Kroger M, Rabin Y and Szleifer I 2011 Morphology control of hairy nanopores *ACS Nano* **5** 4737–47
[45] Kox R, Deheryan S, Chen C, Arjmandi N, Lagae L and Borghs G 2010 Local solid-state modification of nanopore surface charges *Nanotechnology* **21** 335703
[46] Nguyen G, Howorka S and Siwy Z S 2011 DNA strands attached inside single conical nanopores: ionic pore characteristics and insight into DNA biophysics *J. Membr. Biol.* **239** 105–13
[47] Fadeev A Y and McCarthy T J 2000 Self-assembly is not the only reaction possible between alkyltrichlorosilanes and surfaces: monomolecular and oligomeric covalently attached layers of dichloro- and trichloroalkylsilanes on silicon *Langmuir* **16** 7268–74
[48] Howarter J A and Youngblood J P 2006 Optimization of silica silanization by 3-aminopropyltriethoxysilane *Langmuir* **22** 11142–7
[49] Fiorilli S, Rivolo P, Descrovi E, Ricciardi C, Pasquardini L, Lunelli L, Vanzetti L, Pederzolli C, Onida B and Garrone E 2008 Vapor-phase self-assembled monolayers of aminosilane on plasma-activated silicon substrates *J. Colloid Interface Sci.* **321** 235–41
[50] Mussi V, Fanzio P, Repetto L, Firpo G, Stigliani S, Tonini G P and Valbusa U 2011 'DNA-dressed NAnopore' for complementary sequence detection *Biosens. Bioelectron.* **29** 125–31
[51] Repa P, Cespiro Z, Peksa L, Gronych T and Tesar J 1999 Measurement of pressure differences between various positions in a vacuum chamber where pressure is generated dynamically *Metrologia* **36** 551–4
[52] Peksa L, Gronych T, Repa P and Tesar J 2002 Measurement of the pressure differences in a large chamber where the pressure is generated dynamically *Vacuum* **67** 333–8
[53] Raju G G 2006 *Gaseous Electronics: Theory and Practice* (London: Taylor and Francis)
[54] Firpo G, Repetto L, Buatier de Mongeot F and Valbusa U 2009 Focused-ion beam fabrication of nanometer orifices for leak detection *J. Vac. Sci. Technol.* B **27** 2347–51
[55] George A, Knez M, Hlawacek G, Hagedoorn D, Verputten H H J, van Gastel R and ten Elshof J E 2012 Patterning of organosilane molecular thin films from gas phase and its applications: fabrication of multifunctional surfaces and large area molecular templates for site selective material deposition *Langmuir* **28** 3045–52